JOURNAL OF VIROLOGY, May 1986, p. 542–553
0022-538X/86/050542-12$02.00/0

Vol. 58, No. 2

Structural Domains of the Avian Erythroblastosis Virus *erbB* Protein Required for Fibroblast Transformation: Dissection by In-Frame Insertional Mutagenesis

MARY NG AND MARTIN L. PRIVALSKY*

Department of Bacteriology, University of California at Davis, Davis, California 95616

Received 31 October 1985/Accepted 24 January 1986

Avian erythroblastosis virus (AEV) induces erythroblastosis and fibrosarcomas. The viral *erbB* protein is required for AEV-mediated oncogenesis. To explore the structural aspects of the v-*erbB* polypeptide necessary for its oncogenic function, we created a series of small in-frame insertions in different domains of the v-*erbB* oncogene. AEV genomes bearing lesions within the v-*erbB* kinase domain demonstrated a drastically decreased ability to transform avian fibroblasts, establishing a functional role for this structurally conserved oncogene domain. In contrast, mutations in the extracellular domain, between the transmembrane region and the kinase domain, or at the extreme C terminus of the v-*erbB* protein had no effect on AEV-mediated fibroblast transformation. One lesion within the v-*erbB* kinase domain, a 10-amino acid insertion, produced a temperature-sensitive mutant capable of fibroblast transformation at 36°C but not at 41°C, suggesting that small in-frame insertions have general utility for the in vitro creation of conditional mutants.

Avian erythroblastosis virus (AEV) is a retrovirus that induces fibrosarcomas and erythroblastosis in susceptible birds and transforms fibroblasts and erythroid cells in culture to an oncogenic state (9, 14, 22). A single genetic locus within the AEV genome, v-*erbB*, is required for oncogenic transformation of cells of either linkeage and appears to suffice for tumorigenicity (10, 36, 37). The primary translation product of the v-*erbB* gene is a 61,000-molecular-weight polypeptide ($p61^{v\text{-}erbB}$) which is glycosylated in AEV-infected cells to yield several species of higher apparent molecular weight (principally $gp65^{v\text{-}erbB}$, $gp68^{v\text{-}erbB}$, and $gp73^{v\text{-}erbB}$) (4, 18, 19, 30, 31, 33). v-*erbB*-encoded polypeptide species are tightly associated with membranes in infected cells and appear to be synthesized in the rough endoplasmic reticulum, from which they are translocated to smooth and plasma membrane fractions (4, 18, 31).

The amino acid sequence of the v-*erbB* protein has been determined from the nucleic acid sequence of the molecularly cloned v-*erbB* gene (32, 44; M. L. Privalsky, unpublished data). This predicted amino acid sequence, together with biochemical characterizations of the v-*erbB* protein itself, suggest that the v-*erbB* polypeptide is a transmembrane protein, with the (probably glycosylated) N terminus exposed on the extracellular surface of the AEV-infected cell (18, 19, 44). A short transmembrane domain of 23 hydrophobic amino acids follows this external domain and is followed in turn by an intracellular region structurally related to the catalytic domains found in the tyrosine-specific protein kinase family of oncogene proteins (Fig. 1) (32, 44). However, the external, transmembrane, and extreme C-terminal domains of the v-*erbB* protein lack demonstrable sequence relatedness to any other known viral oncogene polypeptides (44; M. L. Privalsky, unpublished data).

The AEV *erbB* gene probably represents a virally transduced copy of the host-cell gene for epidermal growth factor receptor (EGF receptor) (8, 26, 40). The EGF receptor is involved in the regulation of growth and proliferation in many normal, uninfected cells (see reference 20 for a review). The viral *erbB* gene represents a truncated copy of the full-length cellular gene, lacking coding sequences for both N-terminal EGF-binding and C-terminal phosphorylation sites that are present in the normal EGF receptor (26, 40). The absence of these potential regulatory sequences in the v-*erbB* protein may result in aberrant expression and may therefore account for the oncogenic properties of AEV (7, 11, 24, 27, 40).

To better understand the relationship between the structural features, biochemical properties, and oncogenic abilities of the v-*erbB* protein, we generated a series of in-frame insertions in different regions of the v-*erbB* coding domain. We subsequently tested the effect of these genetic lesions on the ability of the v-*erbB* protein to transform avian fibroblasts. We found by this method that the structural integrity of the kinase domain is essential for the ability of the v-*erbB* protein to transform fibroblasts, demonstrating a functional role for this highly conserved amino acid sequence. In contrast, both C and N termini of the v-*erbB* protein can sustain mutations without apparent effect on fibroblast-transforming ability. Our mutagenesis scheme also allowed us to isolate a defined genetic lesion in the v-*erbB* gene that yields a temperature-sensitive transformation phenotype, suggesting that this form of mutagenesis may be of general use in the creation and analysis of conditional mutants.

MATERIALS AND METHODS

Virus and cells. A stock of the AEV ES-4 strain was generously provided by Thomas Graf and was used as a reference positive control for our biological assays of the AEV-transformed phenotype. Chicken secondary cell cultures consisting mainly of fibroblasts were established from 10- to 12-day-old embryos (SPAFAS flock, C/E or C/O). Both infected and uninfected chicken fibroblasts were maintained in medium 199 (GIBCO Laboratories, Grand Island, N.Y.) supplemented with 10% tryptose phosphate broth, 5% bovine serum, 1% heat-inactivated chicken serum, and antibiotics (1 mg of streptomycin per ml, 100 U of penicillin per ml, 2.5 μg of amphotericin B per ml), using a 0.2% bicarbonate–5%

* Corresponding author.

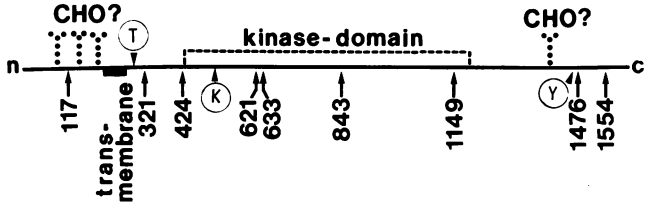

FIG. 1. Schematic of v-*erbB* protein. A linear representation of the AEV strain ES-4 v-*erbB* protein is presented from N terminus (n) to C terminus (c). Regions of possible *N*-linked glycosylation (CHO), the putative transmembrane domain, and the region bearing amino acid sequence relatedness to the tyrosine-specific kinase family of oncogene proteins (kinase-domain) are indicated. Also indicated (by circled letters) are a threonine in the v-*erbB* sequence that may be phosphorylated by protein kinase C (T), a lysine that may represent a portion of the ATP-binding site for the kinase (K), and a tyrosine that can be autophosphorylated in c-*erbB* (Y) (7, 17, 21). Arrows point to *Alu*I restriction sites in the v-*erbB* gene. In this and subsequent figures, the *Alu*I site numbers refer to position of the cleavage site (in base pairs) from the first base of the first methionine codon in the AEV strain ES-4 v-*erbB* open reading frame. The corresponding positions in the numbering system published for the AEV strain H v-*erbB* nucleotide sequence (44) are as follows (strain ES-4/strain H): 117/271, 321/475, 424/578, 621/775, 633/787, 843/997, 1149/1303, 1476/1696, and 1554/1774.

carbon dioxide buffering system (referred to as medium 5 + 1).

Molecular clones. An infectious form of the molecularly cloned AEV DNA genome was kindly supplied by Linda Sealy (36, 37, 42). This infectious plasmid clone (referred to as pAEV-11-3) contains two *Eco*RI restriction endonuclease sites (37). To facilitate manipulation of the plasmid and reconstruction of our mutated subclones into an infectious form, we eliminated the leftmost *Eco*RI site from the pAEV-11-3 plasmid by partial digestion with *Eco*RI, followed by fill-in with Klenow fragment and religation. This process generated the plasmid pAEV-11-3R (containing unique *Sal*I and *Eco*RI sites bracketing the v-*erbB* gene) (Fig. 2).

A subclone of the AEV 2.3-kilobase *Sal*I-*Eco*RI fragment containing the v-*erbB* gene was constructed in pBR322 (pAE-SalRI; Fig. 2) and served as the actual substrate for site-directed mutagenesis, permitting us to mutagenize the v-*erbB* gene in the absence of large amounts of extraneous DNA sequences.

Insertional mutagenesis. We used essentially the procedure of Stone et al. (39) for insertional mutagenesis. Individual molecules of the pAE-SalRI plasmid were linearized at different *Alu*I sites by employing ethidium bromide to limit the restriction endonuclease cleavage reaction (29). The optimal concentration of ethidium bromide was determined empirically: a series of tubes containing supercoiled pAE-SalRI DNA, an excess of *Alu*I, and increasing amounts of ethidium bromide was prepared (2 μg of DNA, 10 U of *Alu*I, and from 0.1 to 20 μg of ethidium bromide in 20 μl of 10 mM Tris chloride [pH 7.5]–50 mM NaCl–10 mM $MgCl_2$ per tube), and the tubes were incubated at 37°C for 2 h. At an ethidium bromide concentration of 1.0 μg/μg of DNA, the supercoiled plasmids were either cleaved or nicked once per molecule before relaxation of the supercoil (and further ethidium bromide binding) prevented additional digestion. A scaled-up digestion of 20 μg of DNA was repeated at the optimal ethidium bromide concentration, and the linearized molecules were separated from nicked circles by preparative gel electrophoresis in low-melting-temperature agarose. The molecules isolated by this procedure represent a heterogeneous, circularly permuted population of plasmids, each linearized at a single *Alu*I site, but with the *Alu*I site cleaved varying from molecule to molecule (Fig. 2).

A 1-μg portion of the *Alu*I-ethidium bromide-linearized DNAs was mixed with 0.1 unit (at an optical density of 260 nm) of a synthetic *Hpa*I linker oligonucleotide (pGTTAAC; obtained from Pharmacia PL Laboratories, N.J.) in 40 μl of ligation buffer (50 mM Tris chloride [pH 7.4], 10 mM $MgCl_2$, 10 mM dithiothreitol, 1 mM spermidine, 1 mM ATP, 100 μg of bovine serum albumin per ml, 2 U of T4 DNA ligase) and incubated for 4 h at 15°C. The ligated plasmids were transformed into competent *Escherichia coli* HB101 cells, and bacteria acquiring plasmids were selected on ampicillin medium. Individual bacterial colonies were propagated, plasmid DNA was isolated, and the site of *Hpa*I linker insertion into the plasmid molecules was determined by restriction endonuclease mapping (unmutagenized pAE-SalRI plasmids do not contain *Hpa*I sites). Eight of the plasmids, bearing insertions in different regions of the v-*erbB* gene, were selected for detailed analysis.

In the method detailed above, the high molar excess of oligonucleotide linkers employed to drive the ligation often resulted in the ligation of multiple linkers at single *Alu*I sites (1). We made a parallel series of single-linker insertions from these polylinker mutants by cleaving each with an excess of *Hpa*I, followed by religation. These single-linker (dipeptide) insertion mutants were tested along with the polylinker mutants for their biochemical and biological properties.

Reconstruction of infectious clones from mutagenized pAE-SalRI subclones. The 2.3-kilobase *Sal*I-*Eco*RI fragments from the various pAE-SalRI plasmid subclones, each bearing *Hpa*I linker insertions in different regions of the v-*erbB* coding domain, were substituted in place of the corresponding wild-type *Sal*I-*Eco*RI fragment in the infectious pAEV-11-3R plasmid (replacing wild-type v-*erbB* sequences with mutated sequences). The resulting AEV genomic plasmids bearing the various v-*erbB* insertional mutations were then transformed into HB101 bacteria and propagated, and the plasmid DNAs were isolated. Retention and stability of the insertional lesions after this procedure was confirmed for each of the mutant infectious plasmids by restriction digestion analysis. A reconstructed wild-type pAEV-11-3R plasmid was also created by the same procedure to confirm the efficacy of our DNA manipulation techniques, employing an unmutagenized pAE-SalRI subclone as the source of v-*erbB* sequences.

Transfection of avian fibroblasts with mutated AEV molecular clones. Approximately 5×10^5 chicken embryo cells were plated into 60-mm tissue culture dishes in medium 5 + 1 and were grown overnight at 39°C. The medium was then replaced with Dulbecco modified Eagle medium (GIBCO) containing 8% fetal bovine serum and 0.2% bicarbonate, and the cells were incubated at 39°C for an additional 4 h before transfection. A 1-μg portion of pAEV-11-3R plasmid DNA (incorporating the insertion lesion desired) was mixed with 0.5 μg of pRAV-10R helper virus DNA (37) and 20 μg of sheared salmon sperm carrier DNA in 0.5 ml of 200 mM $CaCl_2$. An equal volume of 2× HEPES (*N*-2-hydroxyethylpiperazine-*N'*-2-ethanesulfonic acid) buffered saline (HBS; 1.6 g of NaCl, 74 mg of KCl, 39 mg of $Na_2HPO_4 \cdot 7H_2O$, 0.1 g of dextrose, 0.5 g of HEPES [pH 7.05] in 100 ml of water) was slowly added to the DNA-$CaCl_2$ solution, with air bubbling through the mixture to ensure constant agitation. After 10 min at 22°C, 0.5 ml of the resulting calcium phosphate-DNA suspension was added to each 60-mm plate of fibroblasts. The fibroblasts were incu-

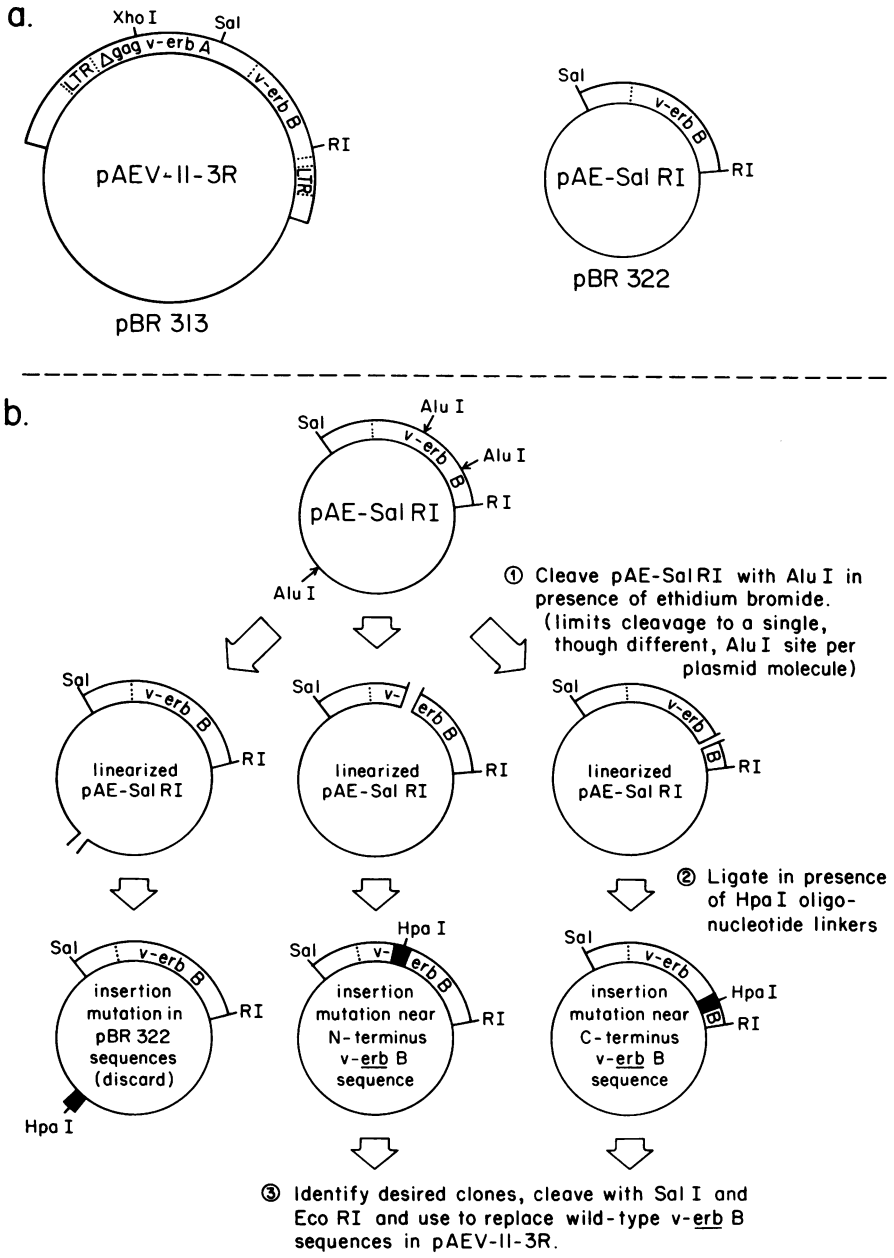

FIG. 2. Construction of v-*erbB* insertion mutants. (A) Plasmid clones employed in the mutagenesis. pAEV-11-3R is an infectious DNA clone of the entire wild-type AEV genome. The long terminal repeats (LTR) and deleted *gag*, v-*erbA*, and v-*erbB* coding regions are shown. pAE-SalRI is a plasmid subclone of the 2.3-kilobase *Sal*I-to-*Eco*RI fragment from the pAEV-11-3R plasmid and consists largely of v-*erbB* sequences. The actual mutagenesis was performed on the pAE-SalRI subclone, and the mutants were subsequently reconstructed into the infectious pAEV-11-3R form. (B) In vitro mutagenesis protocol. The pAE-SalRI plasmid was linearized at different *Alu*I restriction sites, and *Hpa*I hexanucleotide linkers were inserted, as shown schematically for three *Alu*I sites as examples. Sal, *Sal*I restriction site; RI, *Eco*RI restriction site.

bated with the precipitate for 4 h at 39°C, washed, and then treated with 15% dimethyl sulfoxide in HBS for 2 min. The treated cells were washed twice more with medium 5 + 1 and were returned to the 39°C incubator. Once the fibroblasts recovered from the transfection procedure (2 to 3 days), they were passaged 1:5 every 48 h. Cells were assayed for oncogenic phenotype after three to four passages.

Soft-agar colony assay. Transfected fibroblasts were trypsinized and diluted to 10^3 to 10^5 cells per ml of medium 199. The cells were warmed to 45°C and then mixed with 2 volumes of 0.5% agar medium (0.5% Bacto-Agar [Difco Laboratories, Detroit, Mich.] in medium 199 supplemented with 20% fibroblast-conditioned medium) also at 45°C. The agar-cell mixtures were then plated on top of 5 ml of agar medium (1.2% Bacto-Agar in medium 199) already solidified in the bottom of a 60-mm plate. The top agar was allowed to solidify, and the plates were incubated at 39°C for 2 to 3 weeks (feeding at 10-day intervals by overlay of fresh 0.5% agar medium). Incorporation of fibroblast-conditioned medium in these assays (medium 199 from 3-day-old cultures of

chicken embryo secondary cells) abrogated the need for a feeder-cell layer.

Hexose uptake. Cells (10^5) were incubated with 4 μCi of [1-^{3}H]2-deoxyglucose (22 Ci/mmol) for 5 min at 39°C and then were washed extensively, and the cell-associated radiolabel was determined by a liquid scintillation counting technique (34).

Plasminogen-activator protease assay. Fibroblasts transfected by the various v-*erbB* insertion mutations were plated at 5×10^5/60-mm-diameter culture dish and were incubated overnight. The cells were washed once with medium 199 lacking serum, and the plates were overlaid with casein-overlay agar (medium 199 containing 0.4% agarose, 5% chicken serum, antibiotics, and 4% nonfat dry milk) (3, 12). Clear zones of caseinolysis were scored 12 to 16 h later.

Immunoprecipitation analysis of mutant AEV-transfected cells. Monolayers of transfected fibroblasts (approximately 5×10^6 cells per 60-mm culture dish) were pulse-labeled with L-[^{35}S]methionine for 2 h at 39°C as previously described (33). The cells were lysed, and the radiolabeled proteins were analyzed by immunoprecipitation, followed by sodium dodecyl sulfate-polyacrylamide gel electrophoresis. Antiserum to a bacterially synthesized segment of the v-*erbB* protein (anti-bp28$^{v\text{-}erbB}$) was prepared as detailed previously (33).

RESULTS

Set of in-frame insertion mutations created in the v-*erbB* coding region. We employed a method of site-directed mutagenesis on the v-*erbB* gene that has demonstrated great promise in other systems: the creation of a series of small, in-frame insertion mutations (39). DNA sequence analysis revealed that there were nine well-distributed *Alu*I restriction endonuclease sites within the molecularly cloned AEV strain ES-4 v-*erbB* gene (Fig. 1; the corresponding sites in the closely related AEV strain H v-*erbB* gene are also indicated in the figure legend to permit comparison with our ES-4 strain sequence). We therefore used a partial *Alu*I-ethidium bromide digestion to linearize a supercoiled plasmid subclone of the v-*erbB* gene (Fig. 2). We then recircularized the plasmid population in the presence of an excess of hexanucleotide linkers (pGTTAAC). Each hexanucleotide linker introduced in this fashion generated an in-frame insertion at a former *Alu*I site and introduced a novel *Hpa*I recognition sequence at the point of insertion (Fig. 2). Recombinant plasmids bearing *Hpa*I linker insertions at different sites in the v-*erbB* coding domain were identified, subcloned, and propagated.

We were able to isolate eight of the nine possible *Alu*I site insertions (insertions at *Alu*I site 843 were not detected). Of 140 mutagenized plasmid clones analyzed, 54 contained linker insertions in *Alu*I sites in the v-*erbB* coding region, 4 contained insertions in an *Alu*I site upstream of the v-*erbB* coding region (a site not shown in Fig. 1), 75 contained insertions in pBR322-derived sequences, and 7 contained no detectable insertions. The distribution of linker insertions at former *Alu*I sites appeared to be random (there are 14 *Alu*I sites in pBR322-related sequences and 10 *Alu*I sites in AEV-related sequences in the pAE-SalRI subclone), suggesting that the ethidium bromide-limited partial digestion does not introduce a strong bias toward cleavage at any particular *Alu*I restriction site.

The actual sites of the genetic lesions introduced in this manner were confirmed by DNA sequence determination (data not shown). Plasmid clones bearing multimeric linker insertions at a single *Alu*I site (polylinker insertions of four to nine linkers per site) were frequent owing to the high molar excess of oligonucleotides employed during the ligations. These polylinker mutants were analyzed as a set, as were single-linker insertions generated from the polylinkers by *Hpa*I cleavage and religation. We chose to analyze in detail seven of the eight mutants isolated (the *Alu* 633 insertion was not studied because of its proximity to the *Alu* 621 insertion mutation). We will discuss our results with the polylinker mutations first.

Fibroblast transformation by AEV bearing v-*erbB* insertion mutations: substrate-independent growth. The v-*erbB* insertion mutations, created within the pAE-SalRI subclone, were subsequently reconstructed into an infectious form (pAEV-11-3R; Fig. 2). The pAEV-11-3R plasmid contains a complete AEV DNA genome, colinear with the viral RNA genome (36, 37). The reconstructed pAEV-11-3R mutant clones were then introduced into chicken secondary cells by cotransfection in the presence of a helper virus clone (pRAV-10R, an infectious molecular clone of the Rous-associated virus-1 [RAV-1] genome; see reference 37). Replication of input retroviral DNA appears to be required for stable integration in avian cells, and the helper virus clone provides replicative functions that the AEV genome lacks.

Fibroblasts transfected with the various v-*erbB* insertion mutants, with the RAV-1 helper virus alone, or with reconstructed wild-type AEV were first tested for the ability to form colonies in soft-agar medium. Substrate-independent growth is a fairly stringent criterion of oncogenic transformation: normal fibroblasts are unable to propagate in agar suspension, whereas fibroblasts transformed by a number of different agents, including wild-type AEV, are able to replicate and form macroscopic colonies (3, 10, 14, 34, 37).

The results of this assay for the polylinker series of insertion mutations are illustrated in Fig. 3 and 4. Representative microscopic fields of soft-agar plates seeded with cells transfected by the different AEV mutants are shown in Fig. 3. These data are represented quantitatively in Fig. 4. Fibroblasts transfected by wild-type AEV yielded large colonies containing several hundred cells each under these assay conditions (39°C for 2 weeks), whereas fibroblasts transfected by RAV-1 alone failed to give rise to any observable colonies. Viruses with insertional mutations in the extracellular domain of the v-*erbB* protein (*Alu* 117) and between the transmembrane domain and the kinase domain (*Alu* 321) retained full ability to transform fibroblasts by this assay, giving rise to colonies virtually identical in number and morphology to those induced by wild-type v-*erbB*. The same was true of insertions at two sites in the C terminus of the v-*erbB* coding region (*Alu* 1476 and *Alu* 1554). On the other hand, two different mutants bearing insertional lesions in the kinase domain of the v-*erbB* protein (at *Alu* 621 and *Alu* 1149) failed to transform fibroblasts by this criterion, giving rise to drastically reduced numbers of macroscopic colonies (Fig. 4, solid bars). The *Alu* 424-T insertion introduced a nonsense codon into the v-*erbB* sequence; this mutant, as expected, also failed to transform cells (Fig. 3 and 4).

Microscopic examination of these soft-agar cultures revealed that although the *Alu* 621 mutant yielded few macroscopic colonies (colonies of over 100 cells each), this mutant did yield significant numbers of very small colonies of approximately 10 to 20 cells each (Fig. 3 and Fig. 4, dashed bars). This intermediate phenotype at the 39°C assay temperature is due to a temperature-sensitive lesion, as will be discussed in detail later.

Other criteria of fibroblast transformation: hexose uptake.

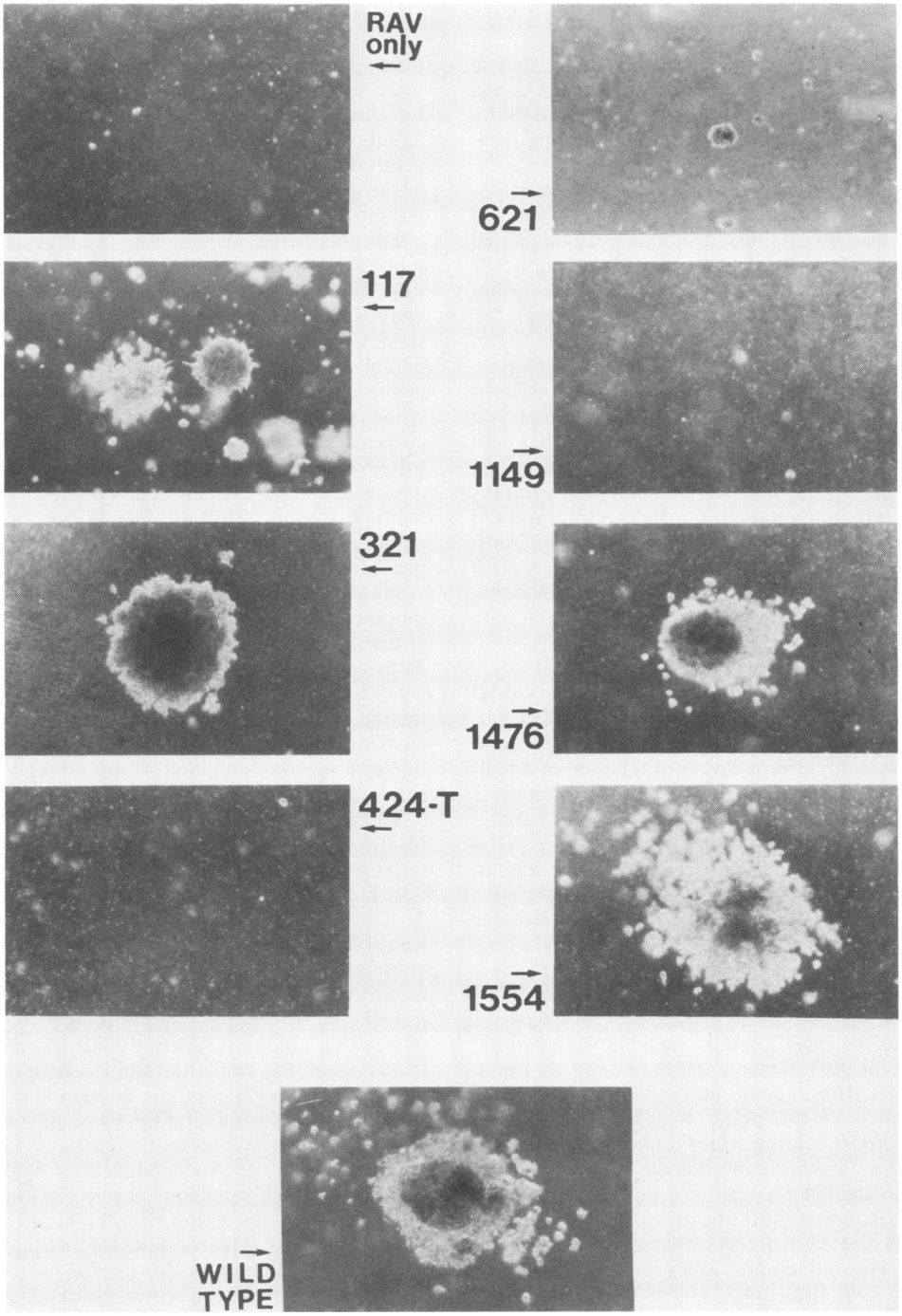

FIG. 3. Soft-agar colonies arising from fibroblasts transfected by different AEV v-*erbB* insertion mutants (polylinker series). Avian fibroblasts transfected by the AEV mutants indicated were seeded into soft-agar medium and incubated for 2 weeks at 39°C. Representative microscopic fields are presented (approximately ×18 magnification). The numbers refer to the position of the insertion in base pairs from the start of the v-*erbB* protein coding region (Fig. 1). The linker insertion into the *Alu* 424 site generates an ochre nonsense codon and a prematurely terminated v-*erbB* protein (Alu 424-T).

Avian fibroblasts transformed by wild-type AEV demonstrate elevated levels of hexose transport (3, 28, 34). We therefore assayed fibroblasts transfected by our various AEV v-*erbB* polylinker insertion mutants for this manifestation of the transformed state (Fig. 5). Fibroblasts transfected by a reconstructed wild-type AEV demonstrated levels of 2-deoxyglucose uptake almost 16-fold greater than those of fibroblasts transfected by helper virus alone. Cells transfected by AEV mutants that were positive in the soft-agar colony assay (*Alu*I sites 117, 321, 1476, and 1554; Fig. 5, solid bars) also possessed high levels of hexose uptake (9- to 14-fold elevated over those of fibroblasts transfected by RAV-1 only). In contrast, fibroblasts transfected by the mutants that were negative in the soft-agar assay (*Alu*I sites

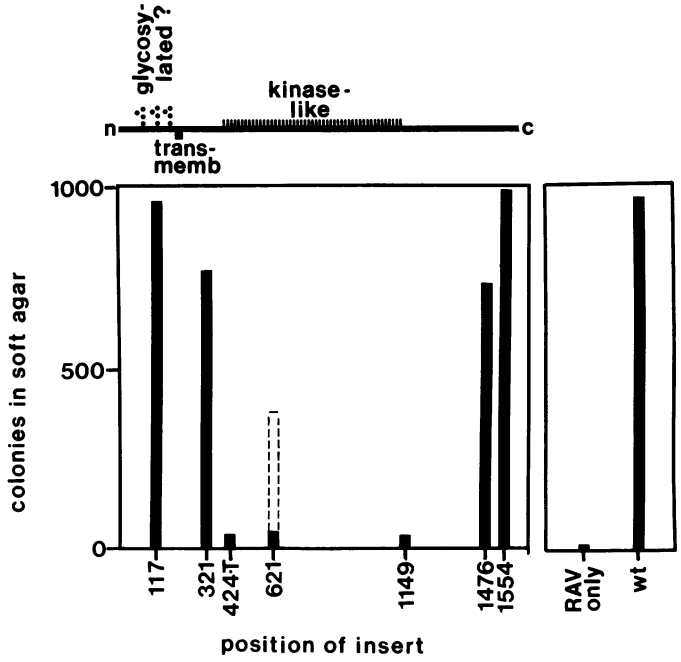

FIG. 4. Soft-agar assay for fibroblasts transfected by different AEV v-*erbB* insertion mutants (polylinker series): quantitation. Fibroblasts transfected by the different AEV v-*erbB* insertion mutants were seeded into soft-agar medium as described in Materials and Methods (10,000 cells per 60-mm culture dish), and the number of cell colonies appearing after 2 weeks at 39°C was determined. The number of fibroblast colonies induced by each AEV insertion mutant is plotted relative to the position of the mutation in the v-*erbB* coding region in base pairs from the beginning of the coding region (below) and relative to a schematic of the v-*erbB* protein (above). Solid lines, Number of large, macroscopic fibroblast colonies; dashed lines, number of small, microscopic fibroblast colonies (see Fig. 3 and the text). Important features of the v-*erbB* protein molecule are indicated as follows: glycosylated?, possible extracellular sites of *N*-linked protein glycosylation; transmemb, transmembrane domain; and kinase-like, v-*erbB* region demonstrating sequence relatedness to the tyrosine kinase family of oncogene proteins. Negative and positive controls included RAV only fibroblasts transfected by the RAV-1 helper virus alone and wt fibroblasts transfected by a reconstructed wild-type AEV. n, N terminus; c, C terminus.

621 and 1149; Fig. 5, open bars) demonstrated much lower levels of 2-deoxyglucose uptake. Hexose uptake by the *Alu* 621 and 1149 mutant-transfected cells was nonetheless three to four times greater than uptake by cells transfected by RAV-1 helper virus alone or by the *Alu* 424-T nonsense mutant (Fig. 5). This general pattern was consistent from assay to assay, with cells from different embryos. These results indicate that even the mutants that are unable to mediate substrate-independent growth may still exert a measurable effect on the phenotype of the transformed cell, perhaps owing to leakiness or to some other phenomenon. This partially transformed phenotype was also observed in the plasminogen activator assay (see below).

Other criteria of oncogenic transformation: plasminogen activator production. Another phenotypic trait that is often associated with oncogenic transformation of fibroblasts is an elevated level of production and secretion of plasminogen activator protease (12). We assayed fibroblasts transfected by the different AEV mutants for protease expression with a casein-agar overlay technique in which the number of

TABLE 1. Plasminogen activator secretion by fibroblasts transfected by AEV v-*erbB* polylinker insertion mutants[a]

Position of insertion	No. of casein hydrolysis plaques
117	280
321	165
424-T	25
621	81
1149	58
1476	512
1554	240
RAV only	21
Wild-type AEV	410

[a] Transfected fibroblasts (5×10^5 in 60-mm tissue culture plates) were washed once with serum-free medium 199 and were overlaid with casein-agarose medium (12). The cells were incubated at 39°C for 16 h, and the clear plaques of caseinolysis were scored.

caseinolytic plaques is proportional to the number of cells secreting plasminogen activator (3, 28). The results for the polylinker series of mutations are presented in Table 1. Fibroblasts transfected by virus bearing insertions in N- and C-terminal regions of the v-*erbB* protein demonstrated a transformed phenotype in this assay, producing caseinolytic plaques comparable in number and size to those induced by wild-type virus. In contrast, mutants with insertions in the kinase domain had drastically lower levels of plasminogen activator secretion. Once again, however, the *Alu* 621 kinase domain mutant produced an intermediate phenotype, con-

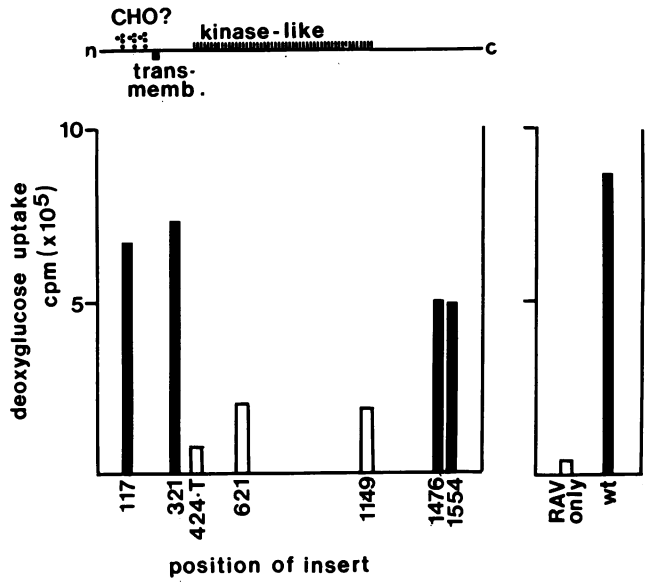

FIG. 5. Hexose uptake by fibroblasts transfected by different AEV v-*erbB* insertion mutants. Fibroblasts transfected by the various AEV v-*erbB* insertion mutants were assayed for the ability to accumulate [^{3}H]deoxyglucose from the medium during a 5-min pulse-label at 39°C, as described in Materials and Methods. The incorporation of isotope per 10^5 cells is plotted for each of the different mutants, relative to the position of the mutation in the v-*erbB* coding region (see the legend to Fig. 4 for an explanation of the abbreviations used). Solid bars, Mutants positive for substrate-independent growth; open bars, mutants negative for substrate-independent growth.

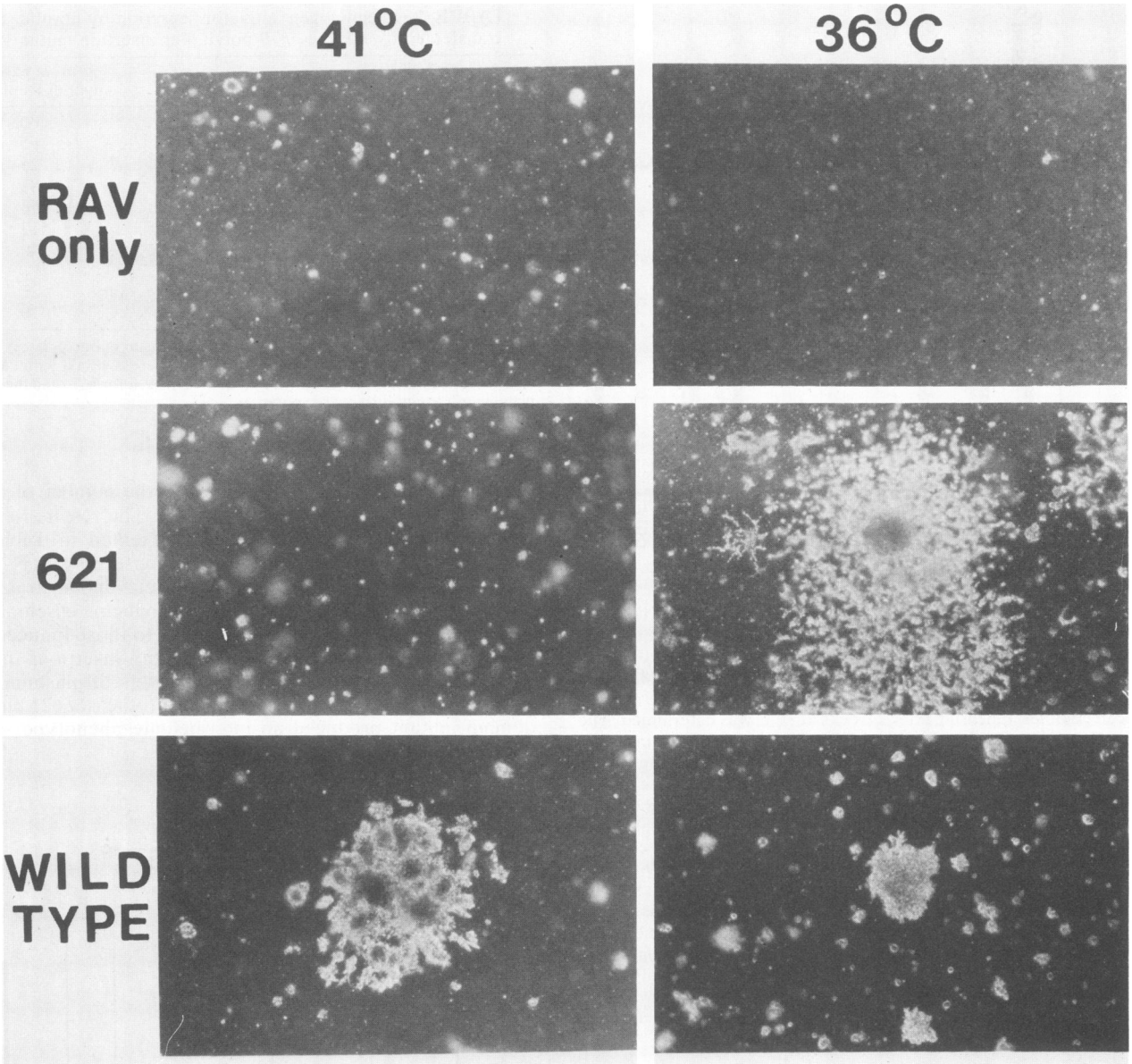

FIG. 6. Fibroblast colonies in soft agar induced by temperature-sensitive *Alu* 621 mutant at 36 and 41°C. Fibroblasts transfected by the *Alu* 621 AEV v-*erbB* insertion mutant were seeded into soft-agar medium as described in the legend to Fig. 3 and incubated at either 36 or 41°C for 2 weeks. Photomicrographs of representative fields are shown (approximately ×25 magnification). Also shown at the same magnification are the results of assays performed in parallel with fibroblasts transfected by the RAV-1 helper virus alone and by a reconstructed wild-type AEV.

sistently demonstrating plasminogen activator levels at 39°C slightly greater than those of helper virus alone.

Polylinker insertions at *Alu*I site 621 yield a temperature-sensitive phenotype. As previously indicated, we noted that certain of the insertion mutations in v-*erbB*, particularly those at the *Alu* 621 site, yielded an intermediate transformed phenotype in a number of different assays performed at 39°C (colony formation in soft agar, deoxyglucose uptake, and plasminogen activator protease secretion). In at least one other system, small in-frame insertion mutations yielded temperature-sensitive protein products (5). Our polylinker mutants with an intermediate phenotype at 39°C were therefore reassayed at both 36 and 42°C. Polylinker insertions into the *Alu* 621 site yielded a strongly temperature-sensitive phenotype, producing soft-agar colonies comparable in size, morphology, and number to those of wild-type AEV when assayed at the permissive temperature (36°C) but yielding few or no colonies at the nonpermissive temperature (42°C) (Fig. 6). We observed the same temperature-sensitive phenotype in fibroblasts transfected by a second, independently derived *Alu* 621 polylinker insertion mutant (data not shown). Deoxyglucose uptake of fibroblasts transfected by the *Alu* 621 polylinker mutants also demonstrated temperature sensitivity. When fibroblasts transfected by these mutants were maintained at 36°C for 1 week before assay, they consistently exhibited hexose uptake rates two- to threefold greater than those of the same cells maintained at 41°C (Table 2). The levels of 2-deoxyglucose uptake exhibited by the *Alu* 621 mutant at 36°C were comparable to those of cells transfected by wild-type AEV (Table 2).

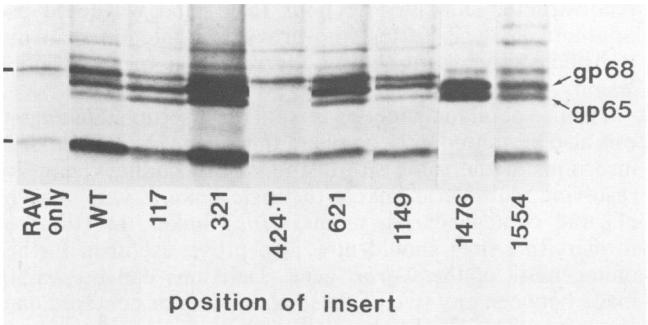

FIG. 7. v-*erbB* proteins synthesized in fibroblasts transfected by different AEV insertion mutants. Mutant-transfected fibroblasts were incubated for 2 h in Dulbecco modified Eagle medium containing 100 μCi of [^{35}S]methionine per ml (3,000 Ci/mmol). The cells were then washed and lysed, and the *erb*-related polypeptides were immunoprecipitated as previously described (33). The immunoprecipitates were analyzed by electrophoresis through a sodium dodecyl sulfate–8% polyacrylamide gel, and the radiolabeled proteins were visualized by autoradiography. The positions on the autoradiogram of the major v-*erbB* protein species synthesized by wild-type AEV during this 2-h pulse-label (65,000 and 68,000 in apparent molecular weight) are indicated. RAV only, Immunoprecipitate of fibroblasts transfected by the RAV-1 helper virus alone; wt, immunoprecipitate of fibroblasts transfected by a reconstructed wild-type AEV. Bars at left point to background proteins not related to v-*erbB*.

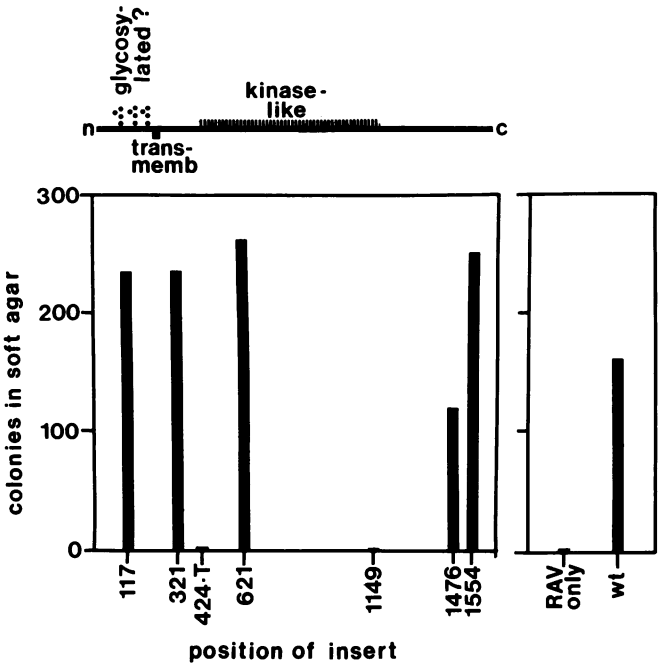

FIG. 8. Soft-agar colony assay for fibroblasts transfected by AEV v-*erbB* single-linker insertion mutants. Fibroblasts transfected by AEV mutants bearing single-linker (dipeptide) insertions at the indicated positions in the v-*erbB* coding region were seeded into soft-agar medium as described in Materials and Methods. Large, macroscopic fibroblast colonies were scored after a 2-week incubation at 39°C (solid bars). Abbreviations are as described in the legend to Fig. 4.

Proviruses and v-*erbB* expression in fibroblasts transfected by AEV insertion mutants. A trivial explanation of our results would be that certain of our insertion mutants could not infect avian fibroblasts or were unable to express wild-type levels of a stable v-*erbB* protein. We also wished to ensure that the phenotypes of the fibroblast cultures analyzed were truly due to the AEV mutant introduced and not due to accidental cross-contamination with wild-type AEV or due to some revertant event. We therefore performed a Southern analysis of each of the mutant-transfected fibroblast lines, cleaving the genomic DNA with *Hpa*I and a number of other restriction endonucleases and analyzing the resulting gel blots with *erb*-specific probes (data not shown). In all cases, the fibroblasts contained integrated AEV proviruses, and these proviruses possessed a genomic structure identical to that of the AEV mutant originally introduced, with no evidence of wild-type viral contamination or detectable proviral rearrangements.

Although Southern analysis confirmed the infectivity and genetic arrangement of our mutant AEVs, it did not address the issue of whether the v-*erbB* gene was expressed. We therefore analyzed the v-*erbB* proteins synthesized by our mutants, utilizing an immunoprecipitation-sodium dodecyl sulfate-polyacrylamide gel electrophoresis analysis (Fig. 7). With the exception of the *Alu* 424-T nonsense mutant, all of the mutant viruses synthesized v-*erbB* protein at levels comparable to or greater than that of wild-type AEV (the gp65$^{v\text{-}erbB}$ and gp68$^{v\text{-}erbB}$ polypeptides were the predominant species produced during this 2-h pulse-label). The *Alu* 424-T insertion should produce a prematurely terminated v-*erbB* polypeptide of approximately 14,000 molecular weight. Unfortunately, our antisera were not reactive against this N-terminal peptide fragment (33), and we did not detect this prematurely terminated v-*erbB* protein in our immunoprecipitates. The v-*erbB* proteins synthesized by our insertion mutants varied slightly in apparent molecular weight from one another and from the wild-type polypeptide, probably owing to the variable number of linker multimers present in the different mutants (four to nine per *Alu*I site).

TABLE 2. Temperature-sensitive hexose uptake in fibroblasts transfected by AEV polylinker mutant 621[a]

Cells	Hexose uptake (cpm) at:	
	36°C	41°C
RAV only	4,500	3,400
621	22,300	11,700
Wild-type AEV	19,700	25,800

[a] Avian fibroblasts transfected by the RAV helper virus alone, by the 621 polylinker insertion mutant, or by wild-type AEV were passaged into duplicate cultures. One aliquot of each cell type was propagated at 36°C; the other aliquot was propagated at 41°C. After 7 days, the cells were assayed for 2-deoxyglucose uptake as described in Materials and Methods and the legend to Fig. 2. The actual uptake assay was performed at 39°C. The data presented are the average of two duplicate determinations performed at each temperature for each cell type.

Analysis of single-linker insertion mutants. The initial genetic lesions created by our mutagenesis scheme consisted of the insertion of multiple, in-frame hexanucleotide linkers at each *Alu*I site (from four to nine linkers, introducing 8 to 18 amino acids into the mutated protein). We desired to reanalyze the effects of these genetic lesions in the context of smaller, single-linker insertions (dipeptide insertions). We therefore digested each of our polylinker insertion mutations to completion with *Hpa*I (removing the extra linkers) and religated the DNA molecules. These single-linker insertion mutations were then reconstructed into an infectious form and transfected into avian fibroblasts, and the cells were characterized for the transformed phenotype as described

TABLE 3. Hexose uptake and plasminogen activator secretion by fibroblasts transfected by AEV v-*erbB* monomeric linker insertions[a]

Site of Insertion	Deoxyglucose uptake (cpm)	No. of casein hydrolysis plaques
117	12,500	219
321	15,900	134
424-T	4,400	0
621	7,900	21
1149	1,700	2
1476	10,000	327
1554	7,073	124
RAV only	3,200	19
Wild-type AEV	9,350	408

[a] Conditions for the measurement of deoxyglucose uptake and plasminogen activator (caseinolysis plaques) were as described in Materials and Methods, the legend to Fig. 5, and Table 1, footnote *a*.

above for the polylinker insertions. The results are indicated in Fig. 8 and Table 3. In general, the results with the single-linker insertions were identical to those already obtained with polylinkers: mutants bearing insertions in the extracellular domain of the v-*erbB* protein, between the transmembrane site and the kinase domain, and in the C-terminal portion of the v-*erbB* coding domain were fully capable of transforming fibroblasts. These results provide an independent confirmation of the data obtained with the polylinker insertions. Single dipeptide insertions at the *Alu* 424-T and *Alu* 1149 sites were unable to transform fibroblasts, a property shared with polylinker insertion mutations at these same sites.

One striking exception was noted from this general pattern. Fibroblasts transfected by AEV bearing a single-linker insertion at the *Alu* 621 site were fully capable of substrate-independent growth in soft agar at 39°C (Fig. 8), whereas AEV bearing a polylinker insertion at this same v-*erbB* site possessed a strongly temperature-sensitive phenotype. Fibroblasts transfected by the *Alu* 621 single-linker insertion mutant also demonstrated a relatively high hexose transport when grown at 39°C (Table 3). It appears that a small insertion at this region of the kinase domain does not seriously disrupt the conformation of the v-*erbB* protein, whereas a larger insertion may destabilize this region sufficiently to make it thermolabile. Fibroblasts transfected by the *Alu* 621 single-linker mutant retained the low levels of expression of plasminogen activator exhibited by the polylinker mutant at the same site (Table 3), consistent with previous work demonstrating that the different phenotypic properties of transformation can be expressed independently of one another (28).

DISCUSSION

Utility of in-frame linker insertions for mapping functional domains in proteins. The use of linker insertions to create a series of genetic lesions within the AEV *erbB* coding domain possessed several advantages. Mutagenesis was readily performed and permitted us, by use of ethidium bromide-limited cleavage, to use restriction endonuclease sites that are present multiple times in the v-*erbB* gene. The use of an oligonucleotide linker that introduced a novel *Hpa*I restriction site into our plasmid clones was helpful in subsequent mapping of the insertion sites. Further, we could easily reconfirm the nature of each mutated plasmid after it was reconstructed into an infectious form, and we could use Southern analysis to test the proviruses integrated in our transfected avian fibroblasts for retention of the genetic lesion.

The use of oligonucleotide linkers for insertional mutagenesis also permitted us to compare the effects of small or large insertions at the same site in the v-*erbB* coding region by resolving multimeric linkers to single linkers. Our bank of plasmid clones bearing unique *Hpa*I linker insertions at former *Alu*I sites should now also prove useful in further mutagenesis of the v-*erbB* gene. Deletions can be readily made between any two of these *Hpa*I sites or centered on a single site. The *Hpa*I linkers can also be employed to create chimeric constructs with other retroviral oncogenes.

Nature of genetic lesions created by insertional mutagenesis. In five of the seven *Alu*I sites studied, the introduction of a single *Hpa*I linker resulted in the creation of a Glx-Val-Asn-Leu sequence from a Glu-Leu or Gln-Leu sequence (*Alu*I sites 117, 321, 621, 1149, and 1476). These insertions represent conservative changes in the nature and hydrophobicity of the amino acid side chains introduced; this particular oligonucleotide linker was chosen for this reason. The insertion of a single *Hpa*I linker at *Alu*I site 1554 changed a Lys-Leu sequence to a Lys-Val-Asn-Leu sequence, and the introduction of an *Hpa*I linker at position 424 changed a Gly-Ala sequence into a Gly-Gly-ochre sequence. Therefore, all the insertion mutations reported here, with the exception of the nonsense codon insertion at *Alu* 424, introduced identical changes at the different sites in the v-*erbB* polypeptide. The different phenotypic effects caused by our different mutants are therefore likely to be due to the site, rather than to the nature of the insertion.

Validity of our assay of the transformed phenotype. Do the phenotypes of the cells transfected by the different AEV mutants accurately reflect the ability of the mutated v-*erbB* gene to induce oncogenic transformation, or can the different phenotypes we observed be explained by differences in transfection efficiency or differences in the ability of the different v-*erbB* mutants to replicate? We believe that the phenotype of the different transfected cultures can be directly attributed to the oncogenic transformation properties of the different mutant v-*erbB* genes. All the transfections were done in parallel for the different mutant and wild-type viruses, using identical quantities of DNA and cells derived from the same chicken embryo. The results of two independent transfection experiments were identical to the results presented here. Our Southern analyses (data not shown) demonstrated essentially equal levels of proviral DNA in the different mutant and wild-type cultures, indicating that all the cultures integrated and maintained equal quantities of viral DNA. Comparable levels of v-*erbB* protein were synthesized in the different transfected cultures. Infectious virus could be recovered in comparable amounts from cultures transfected by all the different v-*erbB* AEV mutants presented here (data not shown), consistent with previous experiments indicating that the function or lack of function of the v-*erbB* protein has no observable effect on the infectivity or propagation of AEV (37).

Insensitivity of v-*erbB* protein function to N- and C-terminal mutations. In-frame insertions in the extracellular domain of the v-*erbB* protein, between the transmembrane domain and the kinase region, and in the extreme C terminus of this polypeptide did not affect the ability of the v-*erbB* protein to transform avian fibroblasts. The results for our C-terminal insertion mutations are in agreement with the phenotype previously reported for a spontaneous mutant of AEV strain

H (AEV-H *td*130 [43]). The AEV-H *td*130 mutant has sustained a deletion in the C terminus of the v-*erbB* protein and is capable of transforming fibroblasts and inducing sarcomas, but demonstrates a severely diminished ability to transform erythroid cells and induce erythroblastosis. We are currently testing our insertional mutants for the ability to transform erythroid cells.

The *Alu* 321 linker insertion is located between the transmembrane site of the v-*erbB* protein and the beginning of the kinase-like domain (Fig. 1). It appears that even large insertions in this region do not diminish the ability of the v-*erbB* protein to transform avian fibroblasts. Apparently an exact distance between the kinase-like region and the plasma membrane is not critical for activity. A corresponding region of the Fujinami virus *fps* oncogene protein can also sustain large insertions without loss of function (39). Perhaps this domain of the tyrosine-specific protein kinases serves simply as a spacer to extend the "catalytic" kinase domain away from the lipid bilayer.

The *Alu* 321 insertion in the v-*erbB* protein is located nine codons downstream from an amino acid (Thr 98 in the viral protein) that may be a target of protein kinase C phosphorylation. Phosphorylation of a conserved threonine in the same region of the cellular EGF receptor inhibits the kinase activity of the receptor, suggesting that this threonine site is involved in modulation of the activity of the c-*erbB* (EGF receptor) protein (21). We did not, however, note any phenotypic consequences resulting from our mutagenesis near this potential regulatory site: the *Alu* 321 mutant transformed fibroblasts in a manner indistinguishable from that of wild-type AEV.

An in-frame insertion in the extracellular domain of the v-*erbB* protein (*Alu* 117) also failed to affect the ability of this protein to transform avian fibroblasts. This mutation, located in the center of three possible sites of protein glycosylation, also had no visible effect on the glycosylation state of the v-*erbB* protein during a 2-h pulse-label (Fig. 7). We have recently created a deletion mutation of the v-*erbB* protein that removes 52 amino acids of the extracellular domain (including the *Alu* 117 site and all three possible glycosylation sites). This deletion mutation produces an unglycosylated v-*erbB* protein that appears to function normally in oncogenic transformation of both fibroblasts and erythroid cells (M. Bassiri and M. L. Privalsky, manuscript in preparation). It would therefore appear that much of the extracellular domain of the v-*erbB* protein is not required for activity and may simply represent a fossil remnant of the transduction event that created the v-*erbB* protein from the cellular EGF receptor.

Requirement of the kinase-like domain of the v-*erbB* protein for fibroblast transformation. Insertions in the central third of the v-*erbB* coding region resulted in a severely diminished ability of the virus to transform fibroblasts. These transformation-defective genetic lesions were in a region of the v-*erbB* protein that demonstrates a strong amino acid sequence relatedness to domains found in the tyrosine-directed protein kinase family of viral oncogene polypeptides (as typified by the Rous sarcoma virus *src* protein [32, 44]). This highly conserved amino acid sequence is thought to define a portion of the catalytic site of these protein kinases (6, 17), an observation consistent with recent demonstrations of a tyrosine-directed protein kinase activity associated with the AEV v-*erbB* protein (11, 24). Our site-directed mutagenesis represents the first demonstration that the structural integrity of this kinase-like domain is essential for the ability of the v-*erbB* protein to transform avian fibroblasts, indicating that the mechanism of action of the v-*erbB* oncogene in fibroblasts may be closely related to that of other members of the *src* family. We are presently assaying our different v-*erbB* mutants for in vitro kinase activity (11).

Isolation of a genetically defined temperature-sensitive mutation in the v-*erbB* protein. In analyzing the properties of our AEV *erbB* insertion mutations, we noted that polylinker insertions at *Alu* 621, although demonstrating a profoundly diminished ability to transform fibroblasts, did yield an intermediate, partially transformed phenotype (very small colonies in soft agar, intermediate levels of deoxyglucose uptake and plasminogen activator) at the usual assay temperature of 39°C. In other systems small in-frame insertions can cause a temperature-sensitive phenotype (for example, see reference 5). When our *Alu* 621 polylinker mutants were assayed at both 36 and 41°C, a strong temperature dependence for transformation was noted. In both the soft-agar colony assay and the deoxyglucose uptake assay, two independently derived *Alu* 621 mutants were fully transforming at the permissive temperature (36°C) and were nontransforming at the nonpermissive temperature (41°C). The temperature-sensitive *Alu* 621 polylinker insertion is in a region of the kinase domain between a putative ATP-binding site (Fig. 1) and more C-terminal sequences possibly involved in the binding of target protein substrates (by analogy to the cyclic AMP protein kinase [2, 6, 17]); this region within the protein kinase domain varies slightly in sequence and length from oncogene to oncogene (15, 16, 23, 25, 32, 38, 41, 44). Notably, single-linker (dipeptide) insertions at this site appeared to retain transforming function at the elevated temperature, suggesting that this region of the kinase domain can accept small insertions without effect on function but that progressively larger insertions destabilize the polypeptide.

A variety of temperature-sensitive AEV mutants have been isolated by traditional in vivo methods (13, 28). It will be of interest to compare the phenotypes of these mutants with that of our *Alu* 621 mutant when the sites of the in vivo genetic lesions are determined.

Our results suggest that the creation of small in-frame insertions may have general utility in the generation of conditional mutants. This would be particularly useful in analysis of gene products for which no conditional mutations have yet been isolated: for example, developmental genes in yeasts or drosophilia, or certain of the recently isolated cellular oncogenes, such as *neu* (35). This technique, applied in a site-specific manner, may also permit temperature-sensitive effects to be directed toward a particular function of a multidomain polypeptide (the catalytic or regulatory domains of growth factor receptors, for example). In addition, systematic alteration of the size and nature of the insertion may allow better understanding of criteria operating in the establishment and maintenance of protein conformation.

ACKNOWLEDGMENTS

We thank Chet Price and Kathryn Radke for extremely helpful discussions and advice, as well as members of the Bacteriology Department for generous support and assistance.

This work was supported by University of California Cancer Research Coordinating Committee funds and by Public Health Service grant CA38823-01 from the National Institutes of Health.

LITERATURE CITED

1. **Bahl, C. P., K. J. Marians, R. Wu, J. Slawinsky, and S. A. Norang.** 1976. A general method for inserting specific DNA

sequences. Gene **1**:81–86.
2. **Barker, W. C., and M. O. Dayhoff.** 1982. Viral *src* gene products are related to the catalytic chain of mammalian cAMP-dependent protein kinases. Proc. Natl. Acad. Sci. USA **79**: 2836–2839.
3. **Beug, H., and T. Graf.** 1980. Transformation parameters of chicken embryo fibroblasts infected with the ts34 mutant of avian erythroblastosis virus. Virology **100**:348–356.
4. **Beug, H., and M. J. Hayman.** 1984. Temperature-sensitive mutants of avian erythroblastosis virus: surface expression of the *erb* B product correlates with transformation. Cell **36**:963–972.
5. **Boeke, J. D.** 1981. One and two codon insertions of bacteriophage f1. Mol. Gen. Genet. **181**:288–291.
6. **Bramson, H. N., N. Thomas, R. Matsueda, N. C. Nelson, S. S. Taylor, and E. T. Kaiser.** 1982. Modification of the catalytic subunit of bovine heart cAMP-dependent protein kinases with affinity labels related to peptide substrates. J. Biol. Chem. **257**: 10575–10581.
7. **Downward, J., P. Parker, and M. D. Waterfield.** 1984. Autophosphorylation sites on the epidermal growth factor receptor. Nature (London) **311**:483–485.
8. **Downward, J., Y. Yarden, E. Mayes, G. Scrace, N. Totty, P. Stockwell, A. Ullrich, J. Schlessinger, and M. D. Waterfield.** 1984. Close similarity of epidermal growth factor receptor and v-*erb* B oncogene protein sequence. Nature (London) **307**:521–527.
9. **Engelbreth-Holme, J., and A. Rothe Meyer.** 1935. On the connection between erythroblastosis (haemocytoblastosis), myelosis and sarcoma in chicken. Acta Pathol. Microbiol. Scand. **12**:352–377.
10. **Frykberg, L., S. Palmieri, H. Beug, T. Graf, M. J. Hayman, and B. Vennstrom.** 1983. Transforming capacities of avian erythroblastosis virus mutants deleted in the *erb* A or *erb* B oncogenes. Cell **32**:227–238.
11. **Gilmore, T., J. E. DeClue, and G. S. Martin.** 1985. Protein phosphorylation at tyrosine is induced by the v-*erb* B gene product in vivo and in vitro. Cell **40**:609–618.
12. **Goldberg, A. R.** 1974. Increased protease levels in transformed cells: a casein overlay assay for the detection of plasminogen activator production. Cell **2**:95–102.
13. **Graf, T., N. Ade, and H. Beug.** 1978. Temperature sensitive mutant of avian erythroblastosis virus suggests a block in differentiation as mechanism of leukemogenesis. Nature (London) **275**:496–501.
14. **Graf, T., B. Royer-Pokora, G. E. Schubert, and H. Beug.** 1976. Evidence for the multiple oncogenic potential of cloned leukemia virus: in vitro and in vivo studies with avian erythroblastosis virus. Virology **71**:423–433.
15. **Groffen, J., N. Heisterkamp, F. H. Reynolds, and J. R. Stephenson.** 1983. Homology between phosphotyrosine acceptor site of human c-*abl* and viral oncogene products. Nature (London) **304**:167–169.
16. **Hampe, A., I. Laprevotte, F. Galibert, L. A. Fedele, and C. J. Scherr.** 1982. Nucleotide sequences of feline retroviral oncogenes (v-*fes*) provide evidence for a family of tyrosine-specific protein kinase genes. Cell **30**:775–785.
17. **Hashimoto, E., K. Takio, and E. G. Krebs.** 1982. Amino acid sequence at the ATP-binding site of cGMP-dependent protein kinase. J. Biol. Sci. **257**:727–733.
18. **Hayman, M. J., and H. Beug.** 1984. Identification of a form of the avian erythroblastosis virus *erb* B gene product at the cell surface. Nature (London) **309**:460–462.
19. **Hayman, M. J., G. Ramsey, K. Savin, G. Kitchener, T. Graf, and H. Beug.** 1983. Identification and characterization of the avian erythroblastosis virus *erb* B gene product as a membrane glycoprotein. Cell **32**:579–588.
20. **Heldin, C. H., and B. Westermark.** 1984. Growth factors: mechanism of action and relation to oncogenes. Cell **37**:9–20.
21. **Hunter, T., N. Ling, and J. A. Cooper.** 1984. Protein kinase C phosphorylation of the EGF receptor at a threonine residue close to the cytoplasmic side of the plasma membrane. Nature (London) **311**:480–482.
22. **Ishizaki, R., and T. Schimizu.** 1979. Heterogeneity of strain R avian (erythroblastosis) virus. Cancer Res. **30**:2827–2831.
23. **Kitamura, N., A. Kitamura, K. Toyoshima, Y. Hirayama, and M. Yoshida.** 1982. Avian sarcoma virus Y73 genome sequence and structural similarity of its transforming gene product to that of Rous sarcoma virus. Nature (London) **297**:205–208.
24. **Kris, R. M., I. Lax, W. Gullick, M. D. Waterfield, A. Ullrich, M. Fridkin, and J. Schlessinger.** 1985. Antibodies against a synthetic peptide as a probe for the kinase activity of the avian EGF receptor and v-*erb* B protein. Cell **40**:619–625.
25. **Mark, G. E., and U. R. Rapp.** 1984. Primary structure of v-*raf*: relatedness to the "*src* family" of oncogenes. Science **224**:285–289.
26. **Merlino, G. T., Y. H. Xu, S. Ishii, A. J. L. Clark, K. Semba, K. Toyoshima, T. Yamamoto, and I. Pastan.** 1984. Amplification and enhanced expression of the epidermal growth factor receptor in A431 human carcinoma cells. Science **224**:417–419.
27. **Nilsen, T. W., P. A. Maroney, R. G. Goodwin, F. M. Rottman, L. B. Crittenden, M. A. Raines, and H. J. Kung.** 1985. c-*erb* B activation in ALV-induced erythroblastosis: novel RNA processing and promoter insertion results in expression of an amino-truncated EGF-receptor. Cell **41**:719–726.
28. **Palmieri, S., H. Beug, and T. Graf.** 1982. Isolation and characterization of four new temperature-sensitive mutants of avian erythroblastosis virus (AEV). Virology **123**:296–311.
29. **Parker, R. C., R. M. Watson, and J. Vinograd.** 1977. Mapping of closed circular DNAs by cleavage with restriction endonucleases and calibration by agarose gel electrophoresis. Proc. Natl. Acad. Sci. USA **74**:851–856.
30. **Privalsky, M. L., and J. M. Bishop.** 1982. Proteins specified by avian erythroblastosis virus: coding region localization and identification of a previously undetected *erb* B polypeptide. Proc. Natl. Acad. Sci. USA **79**:3958–3962.
31. **Privalsky, M. L., and J. M. Bishop.** 1984. Subcellular localization of the v-*erb* B protein, the product of a transforming gene of avian erythroblastosis virus. Virology **135**:356–368.
32. **Privalsky, M. L., R. Ralston, and J. M. Bishop.** 1984. The membrane glycoprotein encoded by the retroviral oncogene v-*erb* B is structurally related to tyrosine-specific protein kinases. Proc. Natl. Acad. Sci. USA **81**:704–707.
33. **Privalsky, M. L., L. Sealy, J. M. Bishop, J. P. McGrath, and A. D. Levinson.** 1983. The product of the avian erythroblastosis virus *erb* B locus is a glycoprotein. Cell **32**:1257–1267.
34. **Royer-Pokora, B., H. Beug, M. Claviez, H. J. Winkhardt, R. R. Friis, and T. Graf.** 1978. Transformation parameters in chicken fibroblasts transformed by AEV and MC29 avian leukemia viruses. Cell **13**:751–760.
35. **Schechter, A. L., D. F. Stern, L. Vaidyanathan, S. J. Decker, J. A. Drebin, M. I. Greene, and R. A. Weinberg.** 1984. The *neu* oncogene: an *erb*-B-related gene encoding a 185,000 M_r tumour antigen. Nature (London) **312**:513–516.
36. **Sealy, L., G. Moscovici, C. Moscovici, and J. M. Bishop.** 1983. Site-specific mutagenesis of avian erythroblastosis virus: v-*erb* A is not required for transformation of fibroblasts. Virology **130**:179–194.
37. **Sealy, L., M. L. Privalsky, G. Moscovici, C. Moscovici, and J. M. Bishop.** 1983. Site-specific mutagenesis of avian erythroblastosis virus: v-*erb* B is required for oncogenicity. Virology **130**:155–177.
38. **Shibuya, M., and H. Hanafusa.** 1982. Nucleotide sequence of Fujinami sarcoma virus: evolutionary relationship of its transforming gene with transforming genes of other sarcoma viruses. Cell **30**:787–795.
39. **Stone, J. C., T. Atkinson, M. Smith, and T. Pawson.** 1984. Identification of functional regions in the transforming protein of Fujinami sarcoma virus by in-phase insertion mutagenesis. Cell **37**:549–558.
40. **Ullrich, A., L. Coussens, J. S. Hayflick, T. J. Dull, A. Gray, A. W. Tam, J. Lee, Y. Yarden, T. A. Liberman, J. Schlessinger, J. Downward, E. L. V. Mayes, N. Whittle, M. D. Waterfield, and P. Seeburg.** 1984. Human epidermal growth factor receptor cDNA sequence and aberrant expression of the amplified gene in A431 epidermal carcinoma cells. Nature (London) **309:**

418–424.

41. **Van Beveren, C., J. A. Galleshaw, V. Jonas, A. J. M. Berns, R. F. Doolittle, D. J. Donoghue, and I. M. Verma.** 1981. Nucleotide sequence and formation of a mouse sarcoma virus. Nature (London) **289**:258–262.
42. **Vennstrom, B., L. Fanshier, C. Moscovici, and J. M. Bishop.** 1980. Molecular cloning of the avian erythroblastosis virus genome and recovery of oncogenic viruses by transfection of chicken cells. J. Virol. **36**:575–585.
43. **Yamamoto, T., H. Hihara, T. Nishida, S. Kawai, and K. Toyoshima.** 1983. A new avian erythroblastosis virus, AEV-H, carries *erb* B gene responsible for the induction of both erythroblastosis and sarcomas. Cell **34**:225–232.
44. **Yamamoto, T., Y. Nishida, N. Miyajimi, S. Kawai, T. Ooi, and K. Toyoshima.** 1983. The *erb* B gene of avian erythroblastosis virus is a member of the *src* gene family. Cell **35**:71–78.